Diffusion Tensor Uncertainty: Visualization and Similarity Metrics

Mustafa Okan Irfanoglu[1,2], Michael Curry[1], Evren Özarslan[1,2], Cheng Guan Koay[1], Sinisa Pajevic[1], and Peter J. Basser[1]

[1]*NIH, NICHD, Bethesda, MD, United States,* [2]*Center for Neuroscience and Regenerative Medicine, Uniformed Services University of the Health Sciences, Bethesda, MD, United States*

Introduction: In order to perform group analyses, particularly in large multi-site studies, there is an increasing need to develop robust and efficient DTI registration schemes. Registration methods that rely only on scalar measures fail to capture the additional directional information content inherent in the diffusion tensor field [2]. Extensions of these approaches that use directional data still do not reflect the underlying data quality and its inherent uncertainty resulting from various sources of noise or from the experimental design. We are proposing a set of distance metrics that enable direct comparisons between estimated mean diffusion tensors in any two voxels, which incorporates the inherent uncertainty of those estimates. We also show novel methods to visualize this uncertainty. Finally, we motivate the use of these metrics to drive whole image tensor field registration, and other applications, like ROI creation, clustering, and segmentation based on statistical hypothesis testing principles.

Materials & Methods:

Data: One healthy subject was scanned with a 3.0T GE Excite MRI using an eight-channel coil. DWI datasets were acquired with FOV= 20 × 23.5 cm, slice thickness = 2 mm, matrix size = 99 × 117, 95 axial slices. DWI data consisted of 10 images with b = 0 s/mm^2, b = 100 s/mm^2, b = 300 s/mm^2 and b = 500 s/mm^2 each, and 30 images with b = 800 s/mm^2 and 50 images with b = 1100 s/mm^2. All DWIs were corrected for motion, eddy-current and EPI distortion. Diffusion tensors were computed using non-linear regression.

Tensor Uncertainty: The estimated diffusion tensor is a function of the underlying tissue and the uncertainty originating from the experimental design and the MRI noise characteristics. Previous work has shown that the mean tensor is distributed according to a multi-variate normal pdf, and the uncertainty of this distribution can be described with a higher order tensor (HOT) containing the covariances among diffusion tensor elements. These HOTs can be computed from the shape of the mean-squared error functional at the optimum solution using error propagation methods.

Uncertainty Visualization: The HOT covariance can be visualized by projecting it onto the unit vector, $r(\theta,\Phi)$. The computed scalar function shows the uncertainty as a function of (θ,Φ) visualized with dense equi-spaced sampling of the unit sphere.

Similarity Metrics: Using the mean and the covariance HOT, we can apply various statistically based metrics to measure distances between different distributions in different voxels in a way that captures the reliability of these tensor measurements. We use the Kullback-Leibler (K-L) divergence. For DTI, with the Normally distributed diffusion tensor, the symmetric K-L measure takes on a simple analytical form:

$$KL\left(N(\gamma_1,\Sigma_1),N(\gamma_2,\Sigma_2)\right)=\left(tr(\Sigma_2^{-1}\Sigma_1)-6\right)+(\gamma_2-\gamma_1)^T\Sigma_2^{-1}(\gamma_2-\gamma_1)$$

where "tr" indicates the trace operator, γ, the vectorized version of a diffusion tensor and ∑ the corresponding covariance matrix.

Results:

Figure 1 shows a familiar ellipsoid map obtained from the diffusion tensor. This axial slice shows the splenium of the corpus callosum, ventricles and gray matter. Figure 2 shows the corresponding uncertainty or covariance surface constructed in the same voxels. Interestingly, even with a large number of gradient directions used, the covariance HOTs do not all appear roughly spherical. Instead, they depend on the anisotropy of the underlying tissue. In isotropic regions, they tend towards spherical shapes whereas in white matter regions their directionality parallels that of the mean tensor, with the highest uncertainty lying along the direction of its primary eigenvector. Additionally, for voxels affected by sub-voxel partial volume contamination at tissue interfaces or for voxels with multiple pathways, the covariance HOTs display more complex multi-lobular shapes.

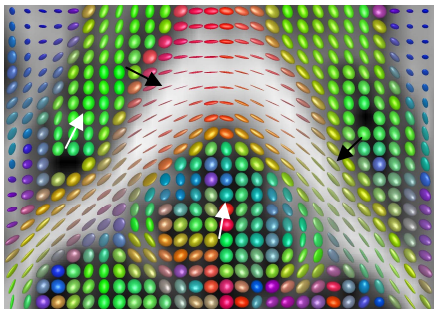

Figure 1. Diffusion tensor ellipsoid map.

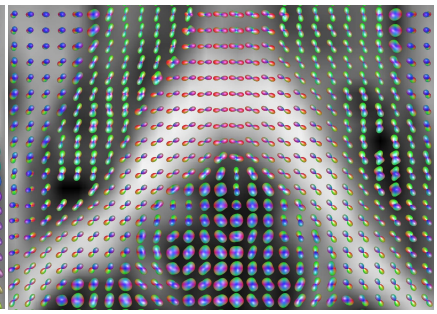

Figure 2. Higher order covariance visualization.

	WM1	WM2	GM	CSF
WM1	0	5.3+ 91	14.7+103	89.2 + 2199
WM2	3 +72.9	0	12.4 + 79	77.6 + 1811
GM	|-3.4| + 19	|-3.1|+ 17	0	21+381
CSF	|-5.3| + 113	-5.2 + 110	-4.5 +81	0

Table 1. K-L divergences between tensor distributions of different tissue types. The metric is able to capture subtle differences such as the increased similarity between WM1 and the less anisotropic voxel WM2 and the gray matter compared to WM1. Additionally, the CSF voxel is the least similar to WM but more similar to GM.

Table 1 shows K-L divergences (as *(tr-6)* + Mahalonobis terms) between and among distributions of mean and covariance HOTs in representative CSF, gray matter, adjacent and distant white matter containing voxels. The K-L divergence captures differences in the size, shape, and orientation of the mean diffusion tensor, but also reflects the uncertainty in the estimates of the mean diffusion tensor.

Discussion: We have presented a method to describe diffusion tensor uncertainty using a novel visualization scheme and proposed a similarity metric that captures the salient features of a complex diffusion tensor field. Additionally, other measures of statistical distance, such as discriminant functions, can now be used in the context of multivariate hypothesis testing to measure relative distances between mean tensors, both within the same tissue regions for ROI generation and for clustering, or between and among different tissue regions, for the purpose of segmentation.

The shape and size of the covariance HOT is a function of the experimental design and image noise in addition to the tissue type. With images with lower SNR, one could expect the trace term of the KL metric to become larger and have a more dominant effect on the divergence. Sparser sampling of the unit sphere with diffusion gradients would also result in more complicated shapes, even in CSF regions. Additionally, for registration and segmentation purposes, it is more suitable to employ the symmetric version of K-L, i.e., "J"-divergence to exhibit metric-like behaviours.

References: **1**. Basser, P. J. et al., JMR, 1994. **2**. Zhang, H. et al. TMI 2007.